RESEARCH ARTICLE

The Effect of Polymer Capping Group to the Electrocatalytic Water Oxidation Activities of Prussian Blue Analogues

Emine ÜLKER* ✉ iD

Recep Tayyip Erdogan University, Faculty of Arts & Sciences, Department of Chemistry, 53100, Rize, Turkey.

Abstract: Prussian Blue (PB) nanoparticles can be obtained by reacting the hexacyanometal center with metal ions in the existence of polymers such as polyethyleneglycol (PEG). In this study, a pentacyanometal complex, $[Fe(CN)_5NO]^{2-}$, was used in addition to hexacyanometal ion, $[Fe(CN)_6]^{3-}$, to obtain nanoparticles coated with PEG. PB nanoparticles have been prepared, characterized, and comprehensive electrochemical studies were performed to investigate their performance for water oxidation electrocatalysis. The effect the ratio of PEG to the morphology and the water oxidation electrocatalytic performance have also been interrogated. Overall, the study clearly indicates that Co-FeNO@PEG with 1:10 and 1:25 Co:PEG rate show the best electrocatalytic activity with an overpotential of 472 and 489 mV for current density of 1 mA cm^{-1}, respectively.

*Corresponding author. E-mail: emine.kapancik@erdogan.edu.tr . **Tel**: +90 (464) 223 6126.

INTRODUCTION

Due to the increasing energy demand and environmental problems based on using fossil fuels, it has been necessary to find alternative energy resources (1). Water splitting is one of the cheap and promising ways to provide environmentally friendly future energy needs (2). There occurs two half reactions: water oxidation (oxygen evolution reaction (OER)) and water reduction (hydrogen evolution reaction (HER)). The OER ($2H_2O \rightarrow 4H^+ + 4e^- + O_2$) is considerably more complex and the rate-limiting step because it requires a 4e$^-$ process. Hence, the robust, efficient and low-cost water oxidation catalysts (WOCs) are necessary to oxidize water with low kinetic overpotential (3).

Although metal oxides such as IrO$_2$ and RuO$_2$ have excellent catalytic activity for OER, their scarcity

and high-cost limit the usability for large-scale applications (4). Therefore, various materials including non-noble 3d metal ions such as metal oxides (5–7), Prussian Blue derivatives (8,9), perovskite structures (10,11) and amorphous materials (12,13) have also been investigated for WOCs with competing activities those of noble-metal catalysts. Because of the high catalytic activities, cobalt oxides stand out among them. However, they are inefficient at neutral or unstable at acidic medium. Furthermore, it is difficult to determine correlation of the catalytic activities with structure due to their amorphous nature (8).

In 2008, Kanan et al. reported that cobalt phosphate (Co-Pi) film easily prepared by electrodeposition of Co^{2+} salts in neutral water containing phosphate as a new area of exploration for non-noble catalysts that oxidize water (14). After this research, many studies have been focus

on Co-Pi catalysts (15–17).

Prussian Blue (PB) structure is a mixed valence iron hexacyanoferrate with a face-centered cubic structure (FCC) that is two different iron centers as Fe^{2+} and Fe^{3+} and CN^- groups that bridge them. Prussian Blue and its analogues draw attention because of their porous structure. Cobalt hexacyanoferrate, members of the well-known Prussian Blue analogue (PBA) family, was coated on fluoride-doped tin oxide (FTO) electrode by electrochemical method and investigated as WOCs by Galán-Mascarós et al (9). This study shows that PBA extraordinary candidates for electrocatalytic WOCs due to their high electrocatalytic activities, robustness, and durability at neutral pH and an alternative to cobalt oxide matrices. Galán-Mascarós et al. also prepared thin films of PBAs with a new synthetic method, which involves chemical etching of cobalt oxides with a hexacyanoferrate solution. This new method provided an impressive improvement on the stability of the electrode and the electrocatalytic performance in a wide pH value(18). Karadas et al. have been investigated electrocatalytic activity of a group of cobalt hexacyanometallates, (CoHCMs) including various $M(CN)_6$ units ($M=Co^{3+}$, Cr^{3+} and $Fe^{2+/3+}$), and impact of the metal and its oxidation state in the $M(CN)_6$ unit on the catalytic efficiencies of PBAs (8). In addition, Karadas shows the cobalt hexacyanocobaltate, as an ideal composition of metal hexacyanocobaltates, exhibits the highest electrocatalytic activity toward the OER (19).

In this study, it is aimed to obtain PB nanoparticles' presences of polyethylene glycol (PEG) as stabilizing agent. The synthesis and characterization of PB nanoparticles@PEG hybrid compounds are presented. Cyclic voltammetric and chronoamperometric studies were performed with catalyst-coated FTO electrode in phosphate buffer (KPi) solution (pH 7). Also, effect of PEG amount on electrocatalytic water oxidation activity was investigated.

EXPERIMENTAL SECTION

Chemicals
All chemicals, including $Co(CH_3COO)_2 \cdot 4H_2O$, $K_4[Fe(CN)_6] \cdot 3H_2O$, $Na_2[Fe[CN]_5NO]$, PEG (used molecular weight of PEG8000), KH_2PO_4 (>99.0%), K_2HPO_4 (>99.0%), orthophosphoric acid (H_3PO_4, 85%), KOH, fluorine-doped tin oxide, and solvents were supplied from Sigma or Merck and used without purification.

Instrumentation
XRD studies were performed by PanAnalytical X'PertPro multipurpose X-ray diffractometer (MPD) operating CuKa radiation (λ=1.5418 Å). FTIR spectra were performed with a Bruker Alpha

Platinum-ATR spectrometer over the wavenumber range 4000–400 cm^{-1}. Dynamic light scattering (DLS) measurements were performed with a photon correlation spectroscopy using a Malvern Nano ZS ZEN3600 (Malvern Instruments Inc.) at a fixed scattering angle of 173° to specify the particle sizes of samples. A transmission electron microscope (TEM, Tecnai G2-F30, FEI) was performed at 200 kV. All electrochemical measurements were carried out by Gamry Instrument Interface 1000 Potentiostat/Galvanostat with a conventional three-electrode electrochemical cell used with Ag/AgCl electrode (satd. KCl) as the reference electrode, Pt as a counter electrode, and catalyst loaded fluorine-doped tin oxide (FTO) as a working electrode. All potentials were reported versus Ag/AgCl reference electrode.

Instrumentation
FTO electrodes were obtained from Sigma-Aldrich (with 1×2 cm, 2 mm slides with 7 Ω/sq^{-1} surface resistivity and $\sim$ 80% transmittance). Electrodes were cleaned by sonication for 10 minutes in basic soapy solution, deionized water and isopropanol, respectively. Then they were annealed at 400 °C for 30 minutes. Catalyst-modified electrodes were prepared by drop-casting method. A mixture of 5 mg of PBA catalyst, 500 µL of DMF, 500 µL of water, and 100 µL of Nafion solution were mixed and sonicated for 30 minutes. After making a stable suspension, 50 µL of it was taken and dropped onto the mixture by covering 1 cm^2 of the FTO electrode. Electrodes were then dried at room temperature for 10 min followed by 80 °C for 10 min in an oven. They were then left in desiccator until further use for electrochemical experiments and characterization.

Electrochemical Methods
Cyclic voltammograms (CV) were recorded with a scan rate of 50 mV s^{-1} in potassium phosphate buffer (KPi) solution with 1M KNO_3 between 0 V and 1.5 V vs Ag/AgCl reference electrode. Surface concentration of active metal site was determined by CV taken in the region of $Co^{2+/3+}$ redox couple with different scan rates. Bulk water electrolysis was performed with a two compartment cell with separation of a glass frit. The electrolysis and steady state chronoamperometric experiments were performed in KPi buffer solution containing 1 M KNO_3 as a supporting electrolyte and the potential was increased with 0.02 V increments to obtain a Tafel plot. Tafel data were collected using equilibrium current density after 600 s at applied potentials. All experiments were performed under nitrogen atmosphere.
Potassium phosphate buffers (0.05 M KPi, pH 7.0) including 1 M KNO_3 were prepared using K_2HPO_4, KH_2PO_4, KNO_3, and deionized water and then set by adding H_3PO_4 or KOH to the desired pH. The

solution was prepared with Millipore Milli-Q deionized water with a resistivity of 18.2 MΩ cm.

RESULTS AND DISCUSSION

Synthesis of Prussian Blue Nanoparticles with PEG

$K_4[Fe(CN)_6].3H_2O$ and $[Fe(CN)_5NO]$ were used as initiators in the presence of $Co(CH_3COO)_2.4H_2O$. The existence of a stabilizing agent prevents the growth of an unlimited number of three-dimensional cyano-bridged coordination polymer networks by providing the formation of metal ions on the surface and stable colloidal (20). Therefore, the particle size was controlled by using PEG as a stabilizing agent of molecular weight of PEG8000. PEG was added to both of two aqueous precursor solutions separately. These two solutions were mixed with each other dropwise until a solid form formation was observed and centrifuged at 9000 rpm for 25 minutes (Figure 1).
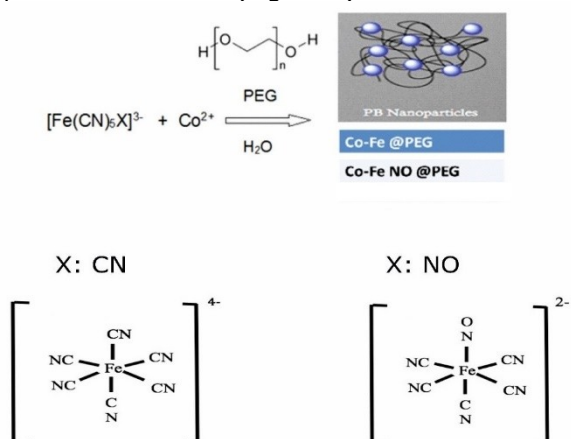

Figure 1. Schematic representation of PBn@PEG formation.

The liquid layer is taken and modest amount of solution pulled away in order to use for DLS measurements. Acetone was added to separate the nano-sized products and stored at 4 °C for a day. Table 1 shows the experimental condition to obtain the structures.

Table 1. Experimental condition to obtain the structures.

Sample	Co/PEG Ratio
Co-Fe@PEG	1/10
Co-Fe@PEG	1/25
Co-FeNO@PEG	1/10
Co-FeNO@PEG	1/25

[1]Co/Fe ratio is 1/1. +
[2]$[Co^{2+}]$ / M = 10^{-2}

Synthesis of Prussian Blue Nanoparticles with PEG

Powder XRD studies were performed on powder samples of derivatives to investigate their crystalline nature. XRD patterns displayed in Figure 2 clearly indicate that all samples adopt identical Prussian Blue nanoparticle structure (20–22).
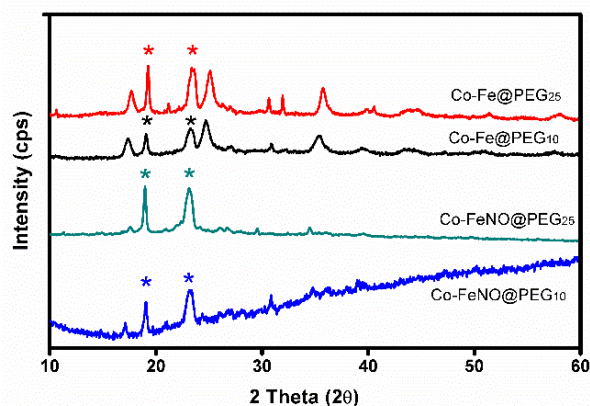

Figure 2. XRD patterns for samples.

PBAs structures exhibit characteristic bands related with PB- structure systems in infrared spectrum: i) HOH bending and OH stretching are observed as a sharp band at around 1610 cm^{-1} and a broad band at 3200– 3500 cm^{-1} respectively. ii) CN stretching is observed as a sharp band at around 2000-2200 cm^{-1}. Therefore, FTIR is one of the reliable techniques for the characterization of PBAs. FTIR spectra of each sample exhibit sharp peak at around 2080 cm^{-1} attributed to CN stretching. Also, each compound has a sharp stretch at around 1580 cm^{-1} and a broad one at 3400 cm^{-1}, which correspond to H-OH bending and O-H stretch, respectively (Figure 3).
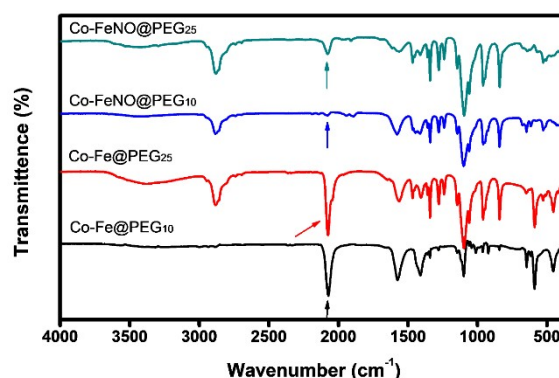

Figure 3. FTIR spectra of the samples.

Dynamic light scattering (DLS) measurements were carried out to specify particle size of Co-Fe@PEG and Co-FeNO@PEG. According to DLS measurements, uniform distribution was observed in the sample and it indicates the formation of particles with diameters of around 15 nm (Figure 4). Transmission Electron Microscopy (TEM) measurements were also performed to determine the size and morphology of the nanoparticles

(Figure 5). The mean particle size for both samples was approximately obtained 20 nm. This result is consistent with DLS measurements.
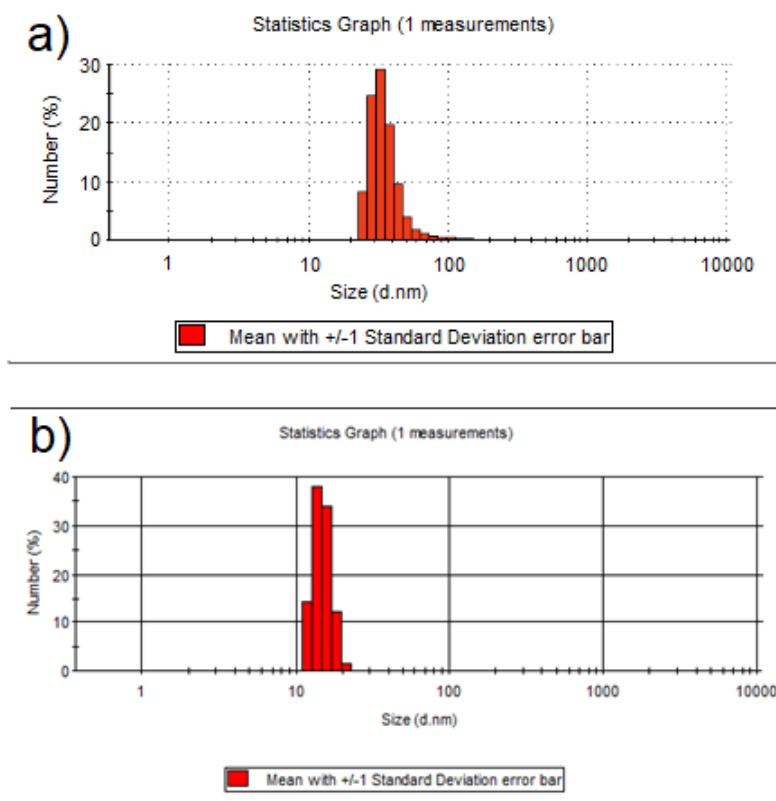

Figure 4. DLS diagrams of a) Co-Fe@PEG b) Co-FeNO@PEG
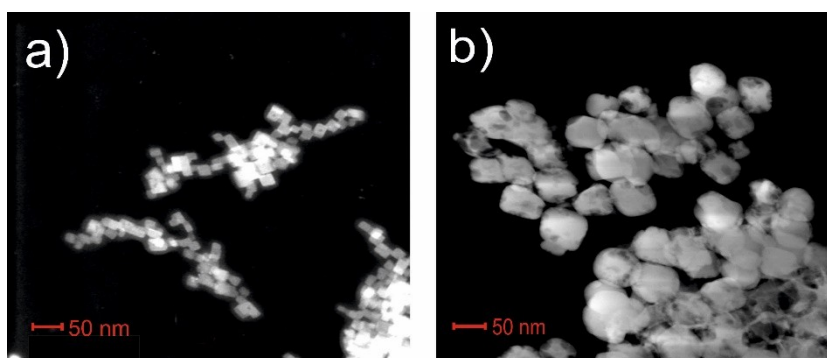

Figure 5. TEM images of **a)** Co-Fe@PEG and **b)** Co-FeNO@PEG

Electrochemical Studies
Electrochemical properties of FTO (PBn@FTO) electrodes coated with Prussian Blue nanoparticles are investigated by cyclic voltammetry (CV) performed in KPi solution (pH 7) containing 1 M KNO_3 as an electrolyte in the range of 0–1.5 V vs. Ag/AgCl reference electrode at a scan rate of 50 mV s^{-1} (Figure 6). All catalysts show the higher irreversible peak attributed to water oxidation process than blank FTO electrode. According to Figure 6a, Co-FeNO@PEG (1:10) exhibits the lowest overpotential, highest current density and thus the highest catalytic activity, among all.

It is also observed that the overpotential value for water oxidation process shifted to more negative regions with the addition of PEG. Figure 6b shows the effect of PEG amount on Co-FeNO catalyst. Co:PEG rate of 1:25 exhibits the best catalytic activity towards the water oxidation.

Both structures exhibit quasi-reversible peaks at around ~ 0.9 V (vs Ag/AgCl), which is attributed to

the $Co^{2+/3+}$ redox process. Redox-active metal concentration on electrode surface was detected by CV performed with various scan rates in the region of $Co^{2+/3+}$ redox couple (19,23). The surface concentrations (Γ) of Co-FeNO@PEG$_{10}$ and Co-FeNO@PEG$_{25}$ were obtained from the slope of current density (j) vs. scan rate plots according to Equation 1:

$$slope = \frac{n^2 F^2 A\Gamma}{4RT} \text{ (Eq. 1)}$$

where n is the number of electrons involved in the redox process, F is the Faraday constant, A is the electrode area, Γ is the electroactive surface concentration, R is the gas constant and T is the temperature. For calculated surface concentration, CVs at different scan rates were recorded at potential ranges of 0.4 V-1.1 V (vs. Ag/AgCl). electroactive surface concentration of Co-FeNO@PEG$_{10}$ and Co-FeNO@PEG$_{25}$ were calculated as 7.8 and 9.3 nmol cm^{-2} (Figure 7). This result suggests that surface concentration of redox-active metal increased with the increase in the amount of PEG.
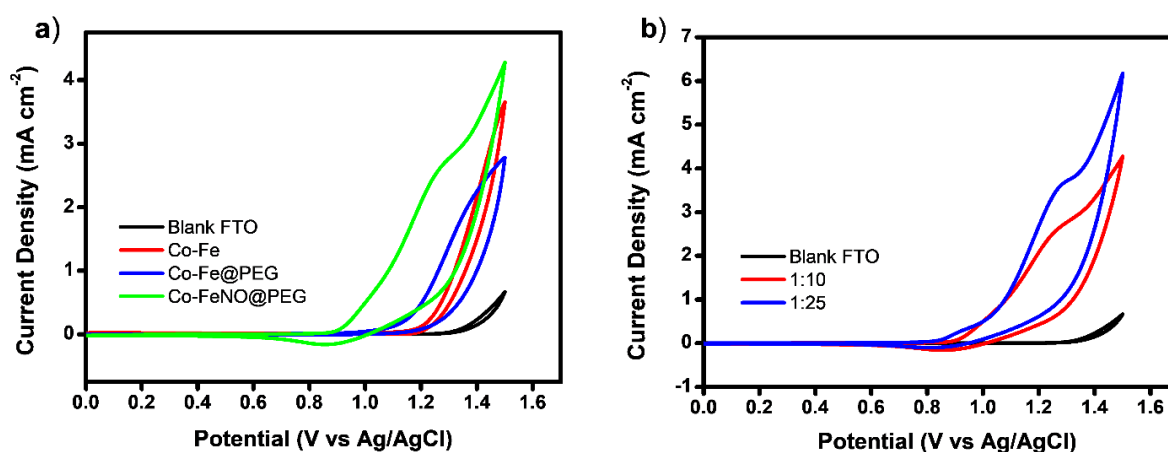

Figure 6. a) CV comparison of PBn modified FTO electrodes at pH 7.0 with a 50 mV s-1 scan rate; b) CV of the Co-FeNO@PEG10 (red line), Co-FeNO@PEG25 (blue line) in the same conditions.

The catalytic activity of the catalysts toward the OER is investigated by corresponding Tafel plots (log j−η) obtained chronoamperometric measurements. The experiments were performed in 50 mM KPi solution with 1 M KNO$_3$ as supporting electrolyte, at pH 7, and the potential was increased with 0.02 V increments to obtain a Tafel slope for each catalysts (Figure 8). A linear trend was obtained in the 280–400 mV region. Tafel slope of Co-FeNO@PEG$_{10}$ and Co-FeNO@PEG$_{25}$ were found to be 96 and 95 mV dec^{-1}, respectively. The similarity in Tafel slopes indicate that the mechanism of water oxidation with these electrodes are similar, however, it is difficult to determine which pathway occurs for the reaction from this analysis. The slopes are similar with previously reported Prussian Blue catalysts (8,9,19), metal dicyanamides [Mdca$_2$] (24), cobalt-sulfide catalyst (25), while it is higher than CoPi catalyst film (26).
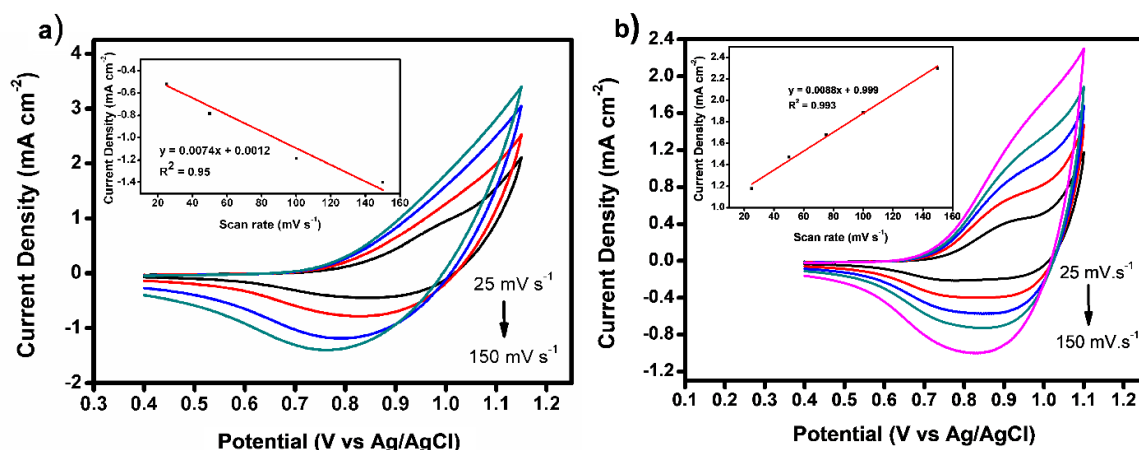
Figure 7. Cyclic voltammograms of a) Co-FeNO@PEG10 and b) Co-FeNO@PEG25 coated FTO electrodes at different scan rates in 50 mM KPi solution containing 1 M KNO$_3$, pH 7; inset shows the linear trend between the scan rate and the Co$^{2+/3+}$ peak current density.

Catalytic current densities of 55 μA cm^{-2} (η_{onset}) and 1 mA cm^{-2} (η_{1mA}) for Co-FeNO@PEG$_{10}$ and Co-FeNO@PEG$_{25}$ were calculated from Tafel linearity as 351, 369, 472 and 489 mV. Onset overpotentials are similar with [CoFe(CN)$_5$-PVP@FTO; 360 mV) (27) and other Co-based catalysts (η: 310 mV for Co(PO$_3$)$_2$, η: 434 mV for Co$_3$O$_4$, and η: 480 mV for CoNCN) (26,28,29). The catalytic onset overpotentials of Co-FeNO@PEG$_{10}$ and Co-FeNO@PEG$_{25}$ are also lower than previous reported [Fe-Co]-coated FTO electrode (η: 475 mV)(19). In addition, catalysts require lower overpotential for 1 mA cm^{-2} than previous reported Prussian Blue catalysts of [CoFe(CN)$_6$@FTO; η > 600 mV] (9), [Co-Co]@ FTO (η: 531 mV), [Co$_{0.9}$Fe$_{0.1}$ -Co]@ FTO (η: 569 mV), [Co0.5Fe$_{0.5}$ -Co]@ FTO (η: 591 mV), [Fe-Co]@ FTO (η: 730 mV) (19) and [CoFe(CN)$_5$-PVP@ FTO; η : 510 mV] (27) fundamentally as a result of the change in the number of active metal sites on electrode surface.

Figure 8. Tafel plots for Co-FeNO@PEG10 and Co-FeNO@PEG25 coated FTO electrode at pH 7.

To further evaluate the catalytic activity of Co-FeNO@PEG$_{10}$ and Co-FeNO@PEG$_{25}$, turnover frequency (TOF) values calculated using surface concentration and current density obtained from chronoamperometric measurement were plotted versus overpotential (Figure 9). TOF of 2 × 10^{-3} s^{-1} can be reached at overpotentials of 251 and 287 mV, respectively. These values are lower than reported for CoFe(CN)$_6$@FTO (η = 300)(9) and Co-Pi catalysts (η = 410)(16), as a result of the surface concentration.
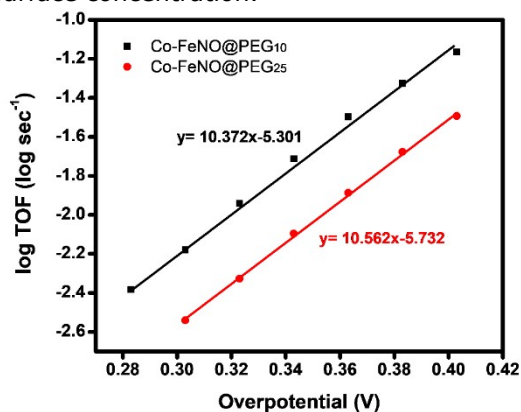

Figure 9. log TOF vs. overpotential plots for Co-FeNO@PEG10 and Co-FeNO@PEG25 extracted from Tafel plots at pH 7.

To determine the long-term stability of Co-FeNO@PEG$_{10}$ and Co-FeNO@PEG$_{25}$ coated FTO electrodes, chronoamperometric measurement was carried out at 1.2 V for 16 hours at pH 7 (Figure 10). The current density increased for the first 2 hours over Co-FeNO@PEG$_{10}$ coated FTO electrode and remained constant at 0.3 mA cm^{-2} during the electrolysis. A beginning increase in the current density can be assigned to morphological changes on the electrode surface like those of previously reported Cu-based catalysts (30,31). Over Co-FeNO@PEG$_{25}$ coated FTO electrode, the current density decreases gradually with time and it stable at 0.2 mA cm^{-1} during the electrolysis. This observation is similar to previous reported Prussian Blue catalysts (9,19).
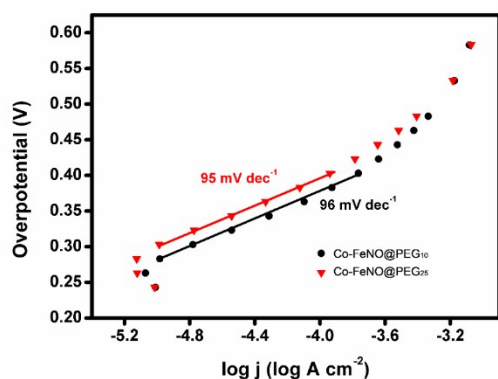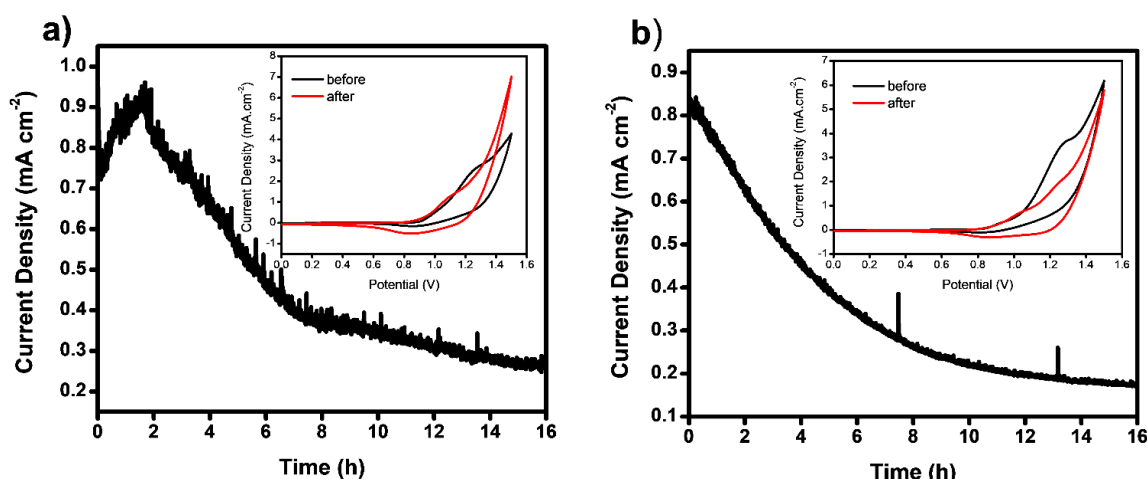
Figure 10. Long-term studies of electrolysis for a) Co-FeNO@PEG10 and b) Co-FeNO@PEG25 coated FTO electrode performed at 1.2 V (vs Ag/AgCl) at pH 7.0. The insets display the CVs obtained pristine and post-catalytic electrode.

In addition, the long-term stability of the catalysts was assessed by comparison of CVs performed before and after 16 hours of electrolysis (Figure 10, inset). An increment in the current density was obtained in the voltammogram of Co-FeNO@PEG$_{10}$ performed after electrolysis, which is consistent with the chronoamperometric measurement. The similarity in the cyclic voltammetric profiles obtained before and after chronoamperometric experiments also supports the stability of both catalysts.

CONCLUSION

Prussian Blue nanoparticles have been synthesized in the presence of PEG as a stabilizing agent, which were used for electrocatalytic water oxidation studies. The effect of the ratio of PEG and the type of cyanide precursor to the electrocatalytic activity were investigated. It is known that the crystallinity of the PB structure decreases formed penta-cyanometal complexes by removing the one CN group from the PB structure, and thus a significant increase in the surface concentration of Co sites. It is observed that the overpotential value for water oxidation process shifted to more negative regions and current density increased by replacing the CN group with the NO group and also with increase in the ratio of PEG, suggesting that surface concentration of redox-active metal increases as a result of increase in the surface area. The current density of 1 mA cm^{-1} was reached at an overpotential of 472 and 489 mV for Co-FeNO@PEG$_{10}$ and Co-FeNO@PEG$_{25}$, respectively. The catalysts offer a TOF = 2×10^{-3} s^{-1} at an overpotential of 262 and 298 mV. The similarity of CVs obtained for the before and after electrolysis suggest the stability of Prussian blue nanocubes during electrocatalysis.

REFERENCES

1. Feng Y, Wei J, Ding Y. Efficient Photochemical, Thermal, and Electrochemical Water Oxidation Catalyzed by a Porous Iron-Based Oxide Derived Metal-Organic Framework. J Phys Chem C. 2016;120:517–26.

2. Zeng M, Wang H, Zhao C, Wei J, Wang W, Bai X. 3D graphene foam-supported cobalt phosphate and borate electrocatalysts for high-efficiency water oxidation. Sci Bull. 2015;60(16):1426–33.

3. Sala X, Romero I, Rodríguez M, Escriche L, Llobet A. Molecular catalysts that oxidize water to dioxygen. Angew Chemie - Int Ed. 2009;48(16):2842–52.

4. Zou X, Su J, Silva R, Goswami A, Sathe BR, Asefa T. Efficient oxygen evolution reaction catalyzed by low-density Ni-doped Co3O4 nanomaterials derived from metal-embedded graphitic C3N4. Chem Commun. 2013;49:7522–4.

5. Smith RDL, Prevot MS, Fagan RD, Zhang Z, Sedach PA, Siu MKJ, et al. Photochemical Route for Accessing Amorphous Metal Oxide Materials for Water Oxidation Catalysis. Science. 2013;340(6128):60–3.

6. Surendranath Y, Dincă M, Nocera DG. Electrolyte-dependent electrosynthesis and activity of cobalt-based water oxidation catalysts. J Am Chem Soc. 2009;131(7):2615–20.

7. Jung S, McCrory CCL, Ferrer IM, Peters JC, Jaramillo TF. Benchmarking nanoparticulate metal oxide electrocatalysts for the alkaline water oxidation reaction. J Mater Chem A. 2016;4(8):3068–76.

8. Alsaç EP, Ülker E, Nune SVK, Dede Y, Karadas F. Tuning the Electronic Properties of Prussian Blue

Analogues for Efficient Water Oxidation Electrocatalysis: Experimental and Computational Studies. Chem - A Eur J. 2018;24(19):4856–63.

9. Pintado S, Goberna-ferro S, Escudero-Adan EC, Galán-Mascarós JR. Fast and Persistent Electrocatalytic Water Oxidation by Co − Fe Prussian Blue Coordination Polymers. J Am Chem Soc. 2013;135:13270–3.

10. May KJ, Carlton CE, Stoerzinger K a., Risch M, Suntivich J, Lee YL, et al. Influence of oxygen evolution during water oxidation on the surface of perovskite oxide catalysts. J Phys Chem Lett. 2012;3(22):3264–70.

11. Kudo A, Kato H, Nakagawa S. Water Splitting into H2 and O2 on New Sr2M2O7 (M = Nb and Ta) Photocatalysts with Layered Perovskite Structures: Factors Affecting the Photocatalytic Activity. J Phys Chem B. 2000;104(3):571–5.

12. Xu L, Zhang F-T, Chen J-H, Fu X-Z, Sun R, Wong C-P. Amorphous NiFe Nanotube Arrays Bifunctional Electrocatalysts for Efficient Electrochemical Overall Water Splitting. ACS Appl Energy Mater. 2018;1:1210–7.

13. Masa J, Weide P, Peeters D, Sinev I, Xia W, Sun Z, et al. Amorphous Cobalt Boride (Co2B) as a Highly Efficient Nonprecious Catalyst for Electrochemical Water Splitting: Oxygen and Hydrogen Evolution (Adv. Energy Mater, 2016, 6, 1502313, 10.1002/aenm.201502313). Adv Energy Mater. 2016;6(12):1502313.

14. Kanan MW, Nocera DG. In situ formation of an oxygen-evolving catalyst in neutral water containing phosphate and Co2+. Science. 2008;321:1072–5.

15. Xie L, Zhang R, Cui L, Liu D, Hao S, Ma Y, et al. High-Performance Electrolytic Oxygen Evolution in Neutral Media Catalyzed by a Cobalt Phosphate Nanoarray. Angew Chemie Int Ed. 2017;56(4):1064–8.

16. Surendranath Y, Kanan MW, Nocera DG. Mechanistic studies of the oxygen evolution reaction by a cobalt-phosphate catalyst at neutral pH. J Am Chem Soc. 2010;132(46):16501–9.

17. Gonzalez-Flores D, Sanchez I, Zaharieva I, Klingan K, Heidkamp J, Chernev P, et al. Heterogeneous water oxidation: Surface activity versus amorphization activation in cobalt phosphate catalysts. Angew Chemie - Int Ed. 2015;54(8):2472–6.

18. Han L, Tang P, Reyes-Carmona A, Rodriguez-Garcia B, Torrens M, Morante JR, et al. Enhanced activity and acid pH stability of Prussian blue-type oxygen evolution electrocatalysts processed by chemical etching. J Am Chem Soc. 2016;138:16037–45.

19. Karadaş F. Investigation of the ideal composition of metal hexacyanocobaltates with high water oxidation

catalytic activity. Turkish J Chem. 2019;43:511–9.

20. Perrier M, Kenouche S, Long J, Thangavel K, Larionova J, Goze-Bac C, et al. Investigation on NMR relaxivity of nano-sized cyano-bridged coordination polymers. Inorg Chem. 2013;52(23):13402–14.

21. Uemura T, Kitagawa S. Prussian blue nanoparticles protected by poly(vinylpyrrolidone). J Am Chem Soc. 2003;125(26):7814–5.

22. Uemura T, Ohba M, Kitagawa S. Size and surface effects of prussian blue nanoparticles protected by organic polymers. Inorg Chem. 2004;43(23):7339–45.

23. Ma M, Qu F, Ji X, Liu D, Hao S, Du G, et al. Bimetallic Nickel-Substituted Cobalt-Borate Nanowire Array: An Earth-Abundant Water Oxidation Electrocatalyst with Superior Activity and Durability at Near Neutral pH. Small. 2017;13(25):1700394.

24. Nune SVK, Basaran AT, Ülker E, Mishra R, Karadas F. Metal Dicyanamides as Efficient and Robust Water-Oxidation Catalysts. ChemCatChem. 2017;9(2):300–7.

25. Sun Y, Liu C, Grauer DC, Yano J, Long JR, Yang P, et al. Electrodeposited cobalt-sulfide catalyst for electrochemical and photoelectrochemical hydrogen generation from water. J Am Chem Soc. 2013;135(47):17699–702.

26. Ahn HS, Tilley TD. Electrocatalytic water oxidation at neutral pH by a nanostructured Co(PO3)2 Anode. Adv Funct Mater. 2013;23(2):227–33.

27. Aksoy M, Nune SVK, Karadas F. A Novel Synthetic Route for the Preparation of an Amorphous Co/Fe Prussian Blue Coordination Compound with High Electrocatalytic Water Oxidation Activity. Inorg Chem. 2016;55(9):4301–7.

28. Biesinger MC, Payne BP, Grosvenor AP, Lau LWM, Gerson AR, Smart RSC. Resolving surface chemical states in XPS analysis of first row transition metals, oxides and hydroxides: Cr, Mn, Fe, Co and Ni. Appl Surf Sci. 2011;257(7):2717–30.

29. Ressnig D, Shalom M, Patscheider J, Moré R, Evangelisti F, Antonietti M, et al. Photochemical and electrocatalytic water oxidation activity of cobalt carbodiimide. J Mater Chem A. 2015;3(9):5072–82.

30. Liu X, Zheng H, Sun Z, Han A, Du P. Earth-abundant copper-based bifunctional electrocatalyst for both catalytic hydrogen production and water oxidation. ACS Catal. 2015;5:1530–8.

31. Mishra R, Ülker E, Karadas F. One-Dimensional Copper(II) Coordination Polymer as an Electrocatalyst for Water Oxidation. ChemElectroChem. 2017;4(1):75–80.